SAN FRANCISCO ESTUARY & WATERSHED SCIENCE
Sponsored by the Delta Science Program and UC Davis Institute for the Environment

RESEARCH

A Note on Conservative Mixing: Implications for Selecting Salinity-Transport Model Constituents in the San Francisco Estuary

Paul H. Hutton[1], Sujoy B. Roy[1*]

ABSTRACT

The deviation of specific electrical conductance (EC) from conservative mixing behavior is well-established in the scientific literature. This principle is based on the observation that, as salt concentration in a water sample increases, the mobility of individual ions in the sample decreases, and thus their ability to conduct electricity decreases. Despite this fact, some commonly used models for salinity transport in the San Francisco Estuary (estuary) utilize EC as a primary simulation constituent, treating it as a conservative quantity. Such a modeling approach has likely been followed to exploit the wide availability of EC data for model calibration and validation, and to obviate the need to translate between EC and salinity in a domain characterized by multiple source waters with varying ionic make-ups. Arguably, this approach provides a reasonable trade-off between data translation error and model simulation error. In this paper, we critically evaluate this approach, employing an extensive salinity data set that includes measurements of EC and major ion concentrations in the estuary. We demonstrate and quantify EC deviation from steady-state, conservative mixing behavior; review the conservative mixing behavior of three bulk salinity measures (practical salinity, ionic strength, and limiting equivalent conductance); and evaluate their source-dependent correlations with EC in the estuary. We find limiting equivalent conductance—a value that assumes uninhibited mobility among individual ions in a water sample—to be an attractive alternative for salinity transport in the estuary. In addition to being a conservative quantity, it is consistently correlated with EC in the estuary's dominant source waters, and thus addresses concerns related to data-translation error. We conclude this paper discussing pros and cons of adopting various salinity-transport model constituents.

KEY WORDS

practical salinity, ionic strength, limiting equivalent conductance, estuarine mixing, salinity transport modeling

INTRODUCTION

Salinity in marine and estuarine waters is typically quantified through measurement of specific electrical conductance (EC), with subsequent conversion to practical salinity using

SFEWS Volume 21 | Issue 2 | Article 3
https://doi.org/10.15447/sfews.2023v21iss2art3

* Corresponding author: sujoy.roy@tetratech.com
1 Tetra Tech, Lafayette, CA 94549 USA

an empirically derived equation proposed by Lewis (1980). The non-linear relationship between EC and salinity captured by this equation is well known from basic physical chemistry: as the ionic concentration of an aqueous solution increases, interactions among ions increase and the marginal effect on conductance decreases. Virtually all models that relate ionic concentrations to EC in natural waters assume a non-linear formulation (e.g., Pawlowicz 2008; review of different methods in McCleskey et al. 2012). Particularly significant at higher ionic strengths, this non-linear effect is consequential in estuarine settings where an expansive salinity gradient from ocean water to riverine water is encountered. Despite this fact, EC is treated as a conservative constituent in some widely used hydrodynamic models developed for the San Francisco Estuary (estuary). This approach is likely to have been implemented for its expediency because the approach obviates the need for converting between EC and salinity during model computation and calibration steps and makes direct use of the widely available EC data in a domain characterized by multiple source waters with varying ionic make-ups. Arguably, this approach provides a reasonable trade-off between data translation error and model simulation error.

The estuary (Figure 1) includes San Francisco Bay, other smaller bays, and an inverted delta (Delta) formed by the Sacramento, San Joaquin, and other smaller rivers that drain California's Central Valley. The Sacramento and San Joaquin rivers are the primary sources of freshwater flow to the estuary, representing more than 90% of the inflows (Fox et al. 1990). The Delta is characterized by a network of channels and islands which have been leveed and developed for agriculture; drainage from these islands provides an internal source of water to the estuary (Fujii 1998). The estuary is home to a vital ecosystem; its inflows and water quality are regulated by the state of California to support co-equal goals of human and natural beneficial uses (DSC 2021). Salinity, which is a fundamental component of the estuary's water-quality regulation, is a function of natural drivers (i.e., mixing of ocean water and freshwater from different parts of the watershed) as well as controllable drivers (notably, water releases from major reservoirs in the upstream watershed and water exports from the Delta). Regulations are focused on managing the timing and magnitude of reservoir releases and Delta exports to achieve different salinity goals over space and time.

Given the significant effects of salinity regulation on the state's economy and ecosystem, a great deal of monitoring and modeling resources have been expended on improving scientific understanding of the estuary (e.g., Hutton et al. 2016; Lund 2016; MacWilliams et al. 2016), and these expenditures are expected to continue into the future. Advancing the state of salinity-transport modeling for the estuary is germane to improving this scientific understanding. In this work, we focus on one specific aspect of salinity-transport modeling by critically examining the effect of treating EC as a conservative constituent. To support this examination, we review the conservative mixing behavior of three bulk salinity measures and discuss the pros and cons of adopting various salinity-transport model constituents.

BACKGROUND

This section introduces the concept of steady-state, two-source, conservative mixing in an estuary and reviews four bulk measures of salinity that are used in this work: ion sum, practical salinity, ionic strength, and limiting equivalent conductance. The latter three quantities are evaluated later in this paper for their usefulness as salinity-transport constituents. Ion sum, on the other hand, is included among the bulk measures as a correlate with EC and the other three bulk salinity measures in evaluating their conservative mixing behavior.

Steady-State, Two-Source, Conservative Mixing

For an idealized estuary with one upstream freshwater inflow, we would expect to observe EC values and ion concentrations that are bounded by the respective upstream freshwater and downstream seawater end-member values; we

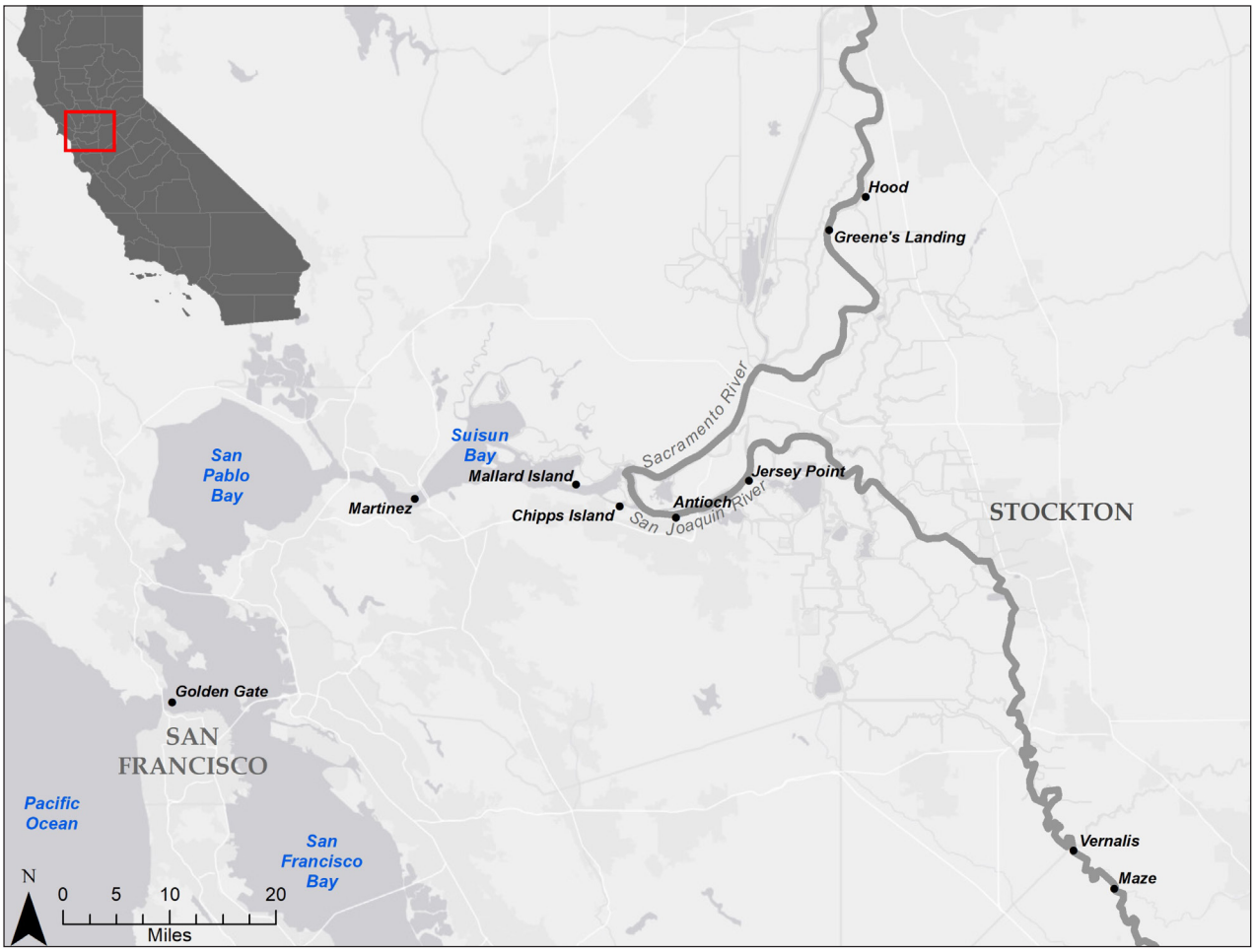

Figure 1 The study area includes San Francisco Bay, other smaller bays, and an inverted delta formed by the Sacramento, San Joaquin, and other smaller rivers that drain California's Central Valley. These hydrographic features, as well as key monitoring locations, are identified in the figure.

would also expect to observe ionic proportions that are characterized by a linear combination (or "mix") of the two sources. Constituent mixing relationships for an estuary can be derived with a single upstream water source—each with two end members—using a linear combination of representative upstream and downstream water sources (Loder and Reichard 1981) for each constituent. Consider the following mixing relationship:

$$S_n = S_s * M_n + S_f * (1 - M_n) \quad (1)$$

where S_n represents the constituent value for a given sample n; S_s and S_f are the end-member constituent values for seawater and freshwater, respectively; and M_n represents the seawater mixing ratio ($0 \leq M_n \leq 1$) for a given sample n. Rearranging terms in Equation 1 and solving for M_n yields:

$$M_n = \frac{S_n - S_f}{S_s - S_f} \quad (2)$$

We expect estuarine water samples associated with a conservative constituent to have a linear relationship with the seawater mixing ratio presented in Equation 2.

Bulk Measures of Salinity

Ion Sum

Direct measurement of major anions and cations in a water sample is an effective, albeit costly method of estimating a water sample's salinity.

https://doi.org/10.15447/sfews.2023v21iss2art3

The ion sum can be defined as the following summation:

$$S = \sum_i C_i \quad (3)$$

where S denotes salinity and C_i is the mass concentration of the i^{th} ionic constituent.

Practical Salinity Scale

The Practical Salinity Scale 1978 or PSS-78 (Lewis 1980) is widely used as a conductivity-based measure of salinity in oceans and estuaries. The scale produces a dimensionless quantity that is defined as a function of a conductivity ratio (sample conductance divided by seawater conductance), temperature, and pressure. The scale, by definition, returns a value of 35 for seawater with a conductivity ratio of unity. Lewis (1980) reports that the scale is valid over the range of 2 to 42. Hill et al. (1986) presents a standard correction to the scale to extend the applicability of PSS-78 below a value of 2. This correction is based on dilutions of standard seawater with pure water, and thus is strictly applicable to waters that have the same proportional ionic make-up as seawater. Hutton and Roy (2023a, 2023b) found the scale to be valid in the study area at practical-salinity values as low as 0.06 (120 µS cm^{-1} EC).

Noting that conductivity data are typically collected in the study area at shallow depths, normalized to a standard temperature of 25 °C, and reported as EC, Schemel (2001) presents the following simplified version of PSS-78, assuming a standard temperature and atmospheric pressure:

$$S = K_0 + K_1 * R^{0.5} + K_2 * R + K_3 * R^{1.5} + K_4 * R^2 + K_5 * R^{2.5} \quad (4)$$

where K_0 = 0.0120, K_1 = - 0.2174, K_2 = 25.3283, K_3 = 13.7714, K_4 = - 6.4788, K_5 = 2.5842, $\sum K$ = 35, and R is the conductivity ratio. Although we acknowledge conceptual and quantitative differences between PSS-78 and ion sum (Millero et al. 2008), we denote both quantities with the same nomenclature S in this work.

Ionic Strength

Ionic strength (Lewis and Randall 1921), an established measure of the intensity of the electrostatic field in a water sample, is defined as the summation:

$$I = \frac{1}{2} * \sum_i \left(\frac{C_i}{MW_i} * Z_i^2 \right) \quad (5)$$

where I is the ionic strength, C_i is previously defined, MW_i is the molecular weight of the i^{th} ionic constituent in a water sample, and Z_i is the valence of the i^{th} ionic constituent. Values of molecular weight and valence are summarized for each of the major ions in Table 1. Lind (1970) showed correlation between EC and ionic strength for synthetic salt solutions as well as a variety of natural waters.

Limiting Equivalent Conductance

Conductivity of a water sample is related to the sum of the concentration and mobility of the free ions in that sample (Miller et al. 1988). McCleskey et al. (2012) reviewed the capability of eleven methods to calculate the conductivity of natural waters from their chemical composition. Here, we refer to the computed conductivity of a water sample as its "limiting equivalent conductance" and define it as the following summation according to Kohlrausch's Law (Miller et al. 1988):

$$\kappa = \sum_i \alpha_i * \lambda_i * C_i \quad (6)$$

where κ is the limiting equivalent conductance of a water sample, α_i is the fraction of the i^{th} ionic constituent present as the free ion, λ_i is the limiting equivalent conductance of the i^{th} ionic constituent, and C_i is previously defined. Ion-specific values for α and λ are summarized in Table 1. As discussed by Miller et al. (1988), the limiting equivalent conductance of an ionic constituent is the "… conductance of an ionic constituent extrapolated to infinite dilution, where interaction between ions in solution disappear and the mobility of individual ions reaches a maximum." We note that, while the nomenclature "limiting equivalent conductance" is typically restricted to an individual ion, we also

Table 1 Ion-specific constants for calculation of ionic strength (see Equation 5) and limiting equivalent conductance (see Equation 6)

Ion constituent	MW (mg mmole^{-1})	Valence Z	α	λ (μS cm^{-1} per mg L^{-1})
Br^-	79.90	–1	0.99	0.98
Cl^-	35.45	–1	0.99	2.15
SO_4^{2-}	96.06	–2	0.93	1.66
HCO_3^-	61.02	–1	0.98	0.73
Na^+	22.99	+1	0.98	2.18
Ca^{2+}	40.08	+2	0.88	2.97
Mg^{2+}	24.31	+2	0.88	4.36
K^+	39.10	+1	0.98	1.88

apply it in this work to a mixed salt sample. In dilute natural waters, κ is a good approximation of measured EC. However, as the concentration of a sample increases and ionic mobility decreases, κ overestimates measured EC. As shown later, κ provides a conservative, albeit theoretical quantity with possible merit as a salinity-transport constituent.

METHODS

Data: Units of Measurement, Sources, Screening and Filling

We used grab sample data collected from the dominant source waters in the study area to evaluate EC deviations from steady-state, conservative mixing behavior and to demonstrate conservative mixing behavior associated with bulk salinity measures previously identified (see "Background"). In addition to specific conductance (EC), these data included concentrations of major ions such as the anions bromide (Br^-), chloride (Cl^-), sulfate (SO_4^{2-}) and alkalinity, and the cations sodium (Na^+), calcium (Ca^{2+}), magnesium (Mg^{2+}), and potassium (K^+). EC values are reported in SI units of microsiemens per cm (µS cm^{-1}), and ion concentrations are generally reported in concentration units of milligrams per liter (mg L^{-1}). Alkalinity data are reported as mg L^{-1} of calcium carbonate.

These data were collected and continue to be collected by the California Department of Water Resources (CDWR) in support of its Municipal Water Quality Investigations Program (Hutton et al. 2022). A subset of these grab sample data was compiled from CDWR's Water Data Library (*http://www.water.ca.gov/waterdatalibrary/*) to represent dominant source waters of the study area, including saline waters in the western Delta and downstream bays, freshwater inflow from the Sacramento River, inflow from the San Joaquin River, and return flows from in-Delta agriculture (i.e., Delta agricultural drainage).

Denton (2015) notes that the quality of salinity grab sample data in the study area is generally very good, and the robustness of correlations between various ionic constituents and EC at many locations within the study area allows for easy identification of data outliers and errors. In this work, we adhered to the following protocol to screen outliers:

- We checked grab sample data for "testability." A testable data sample was defined as one that had a measured value for EC, total dissolved solids (TDS), Cl^-, SO_4^{2-}, Na^+, and Mg^{2+}. We enforced testability to ensure that samples were generally mass- and charge-balanced.

- After the check for "testability," we imposed two additional screening criteria: (1) we removed a data point associated with a single constituent if—when plotted against EC or TDS—it fell outside the 99% prediction band (three standard errors) for the testable set of observations for that constituent, and (2) we removed an entire sample—including all data points associated with it—if three or more constituents in that sample fell outside the 95% prediction band (two standard errors) for the testable set of observations for the constituents.

The above protocol is based on the assumptions that, while total salinity can exhibit unusual behavior under extreme hydrologic conditions, (1) relationships between individual constituents and total salinity exhibit consistent behavior, and (2) major departures from these relationships indicate outlier behavior. Table 2 summarizes the number of screened data points by monitoring

https://doi.org/10.15447/sfews.2023v21iss2art3

Table 2 Number of specific conductance and ion data points by monitoring location

EC/Ion	Western Delta and downstream bays				Sacramento River (Sac R)			San Joaquin River (SJR)				Agricultural drainage
	Sac R @ Mallard	Sac R @ Chipps	SJR @ Jersey	Σ	Sac R @ Hood	Sac R @ Greene's	Σ	SJR near Vernalis	SJR @ Maze	SJR near Vernalis	Σ	Various locations
	1986–2019	2019–2019	1990–1995		1982–2020	1983–1998		1982–2005	1988–1994	2005–2020		1990–2001
EC	382	3	20	405	445	156	601	341	62	140	543	781
Br^-	335	3	20	358	297	80	377	280	38	140	458	781
Cl^-	381	3	20	404	444	154	598	339	62	140	541	781
SO_4^{2-}	377	3	20	400	444	151	595	340	62	140	542	781
Alkalinity	376	3	20	399	438	153	591	340	61	140	541	781
Na^+	378	3	20	401	442	152	594	338	59	140	537	781
Ca^{2+}	379	3	20	402	441	155	596	338	56	140	534	781
Mg^{2+}	374	3	20	397	442	154	596	338	60	140	538	781
K^+	377	3	20	400	436	155	591	330	61	139	530	781

location; this table also indicates the periods in which these data were collected.

We filled missing ion concentration data using previously developed regression relationships with EC (Hutton, Sinha, and Roy 2022) to allow for calculation of mass-based salinity concentrations for comparison with conductivity-based measures of salinity. The filling exercise resulted in the following number of samples by region: 405 samples for the western Delta and downstream bays, 601 samples for the Sacramento River, and 543 samples for the San Joaquin River. The agricultural drainage data set included 781 samples, none of which were filled. As Table 2 reveals, filling contributes a small proportion of ion data to the samples, with Br^- being the exception (e.g., 85 of the 543 San Joaquin River values were filled). We note that, given the low concentration of Br^- relative to total salinity concentration, errors introduced through the filling process are considered negligible.

Calculation of Mass-Based Salinity (Ion Sum)

Salinity concentrations (C_i) were calculated as the sum of the eight major ions described above. As part of this calculation, we converted alkalinity data to equivalent concentrations of bicarbonate (HCO_3^-) in mg L^{-1} by multiplying the former by 1.22 (Hem 1985). Further, these equivalent HCO_3^- concentrations were decreased by a gravimetric factor (mg L^{-1} HCO_3^- × 0.4917 = mg L^{-1} CO_3^{2-}), assuming that roughly half the bicarbonate is volatilized as carbon dioxide and water, and the computed CO_3^{2-} value is used in the salinity calculation. As noted by Hem (1985), the resulting salinity calculation corresponds to the conditions that would exist in the dry residue of a TDS measurement. Finally, we converted ion sum from mg L^{-1} to parts per thousand (ppt) by accounting for sample density, where seawater density at 25 °C was assumed to be 1.024 and pure water was assumed to be 1.000 (Riley and Skirrow 1965). Salinity associated with the screened and filled samples from the western Delta and downstream bays ranged from 0.06 to 10.89 ppt. Similarly, screened and filled salinity samples associated with the Sacramento River, San Joaquin River, and Delta agricultural drainage ranged from 0.04 to 0.13 ppt, 0.06 to 0.99 ppt, and 0.07 to 1.78 ppt, respectively.

Calculation of Other Bulk Measures of Salinity

We computed PSS-78 from measured EC using Equation 4. Hutton and Roy (2023a, 2023b) proposed corrections to the scale for the San Joaquin River and agricultural drainage; however, these corrections were not used in this work. We computed ionic strength in units of millimoles per liter (mM) from measured ionic mass concentrations using Equation 5 and constants presented in Table 1. Finally, we computed

limiting equivalent conductance in units of μS cm^{-1} from measured ionic mass concentrations using Equation 6 and constants presented in Table 1.

Simulation of Salinity Transport with DSM2

CDWR's Delta Simulation Model 2 (DSM2) (CDWR 2022) is a commonly used one-dimensional hydrodynamic model for the estuary. The model's dispersion factors are calibrated with measured EC data, and thus are hypothesized to be biased because of the non-conservative behavior of EC. We conducted several salinity-transport simulations with Version 8.2.1 of this model to evaluate practical limitations of using EC as a conservative salt-calibration parameter. Specifically, we simulated transport of EC, ionic constituents and TDS for the historical hydrologic period of record that spanned October 1, 1999 through December 31, 2017, and compared simulated relationships between salinity constituents with measured relationships at various locations in the estuary.

RESULTS

Deviation of EC from Steady-State Conservative Mixing

Figure 2 plots M_n as a function of ion sum. This figure overlays measured EC data as a function of ion sum, with EC scaled on the secondary ordinate assuming steady-state conservative mixing according to Equation 2. For example, M_n = 0.40 corresponds with EC = 21.07 mS cm^{-1} if EC is assumed to mix conservatively. Assumed end-member values are provided in Table 3. The resulting chart shows that measured EC data falls above the mixing line in a non-linear manner, signifying deviation from conservative behavior (Warner 1972; Loder and Reichard 1981; Patra et al. 2012). A measured ion sum of 6 ppt represents a seawater mixing ratio of approximately 0.17 and a measured EC of approximately 10,500 μS cm^{-1}. However, assumption of conservative mixing corresponds with a mixing ratio of approximately 0.20 at that EC value. Thus, using EC as a measure of transport in the estuary artificially amplifies the actual seawater mixing ratio. Or, said another way, it suppresses the dilution effect associated with freshwater flows to the estuary.

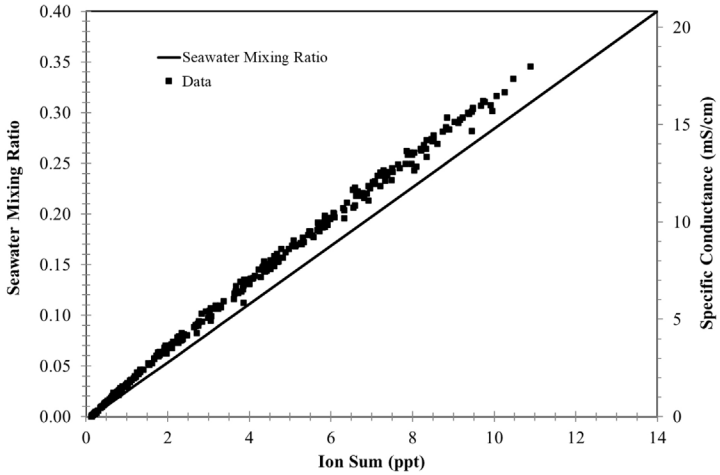

Figure 2 Seawater mixing ratio vs. ion sum. The chart overlays measured specific conductance data (mS cm^{-1}) as a function of ion sum.

Table 3 End-member values

Bulk salinity measure	Units	Downstream value (seawater)	Upstream value (freshwater)
Ion sum	ppt	34.33	0.130
Specific electrical conductance	μS cm^{-1}	52,300	250
Practical salinity	dimensionless	35.00	0.122
Ionic strength	mM	697.1	3.3
Limiting equivalent conductance	μS cm^{-1}	75,636	259

Conservative Mixing Behavior of Bulk Salinity Measures

Figure 3, similar to Figure 2, plots M_n as a function of ion sum. The top, middle, and bottom panels of the figure overlay computed values of practical salinity, ionic strength, and limiting equivalent conductance as functions of measured ion sum, with each bulk salinity measure scaled on the secondary y-axis assuming steady-state conservative mixing. Assumed end-member values associated with the mixing plots are provided in Table 3. M_n = 0.40 corresponds with S = 14.07, I = 280.8 mM, and κ = 30.41 mS cm^{-1} if these bulk salinity measures are assumed to mix conservatively according to Equation 2. Figure 3 shows each of the three measures falling along the mixing line, signifying conservative behavior.

https://doi.org/10.15447/sfews.2023v21iss2art3

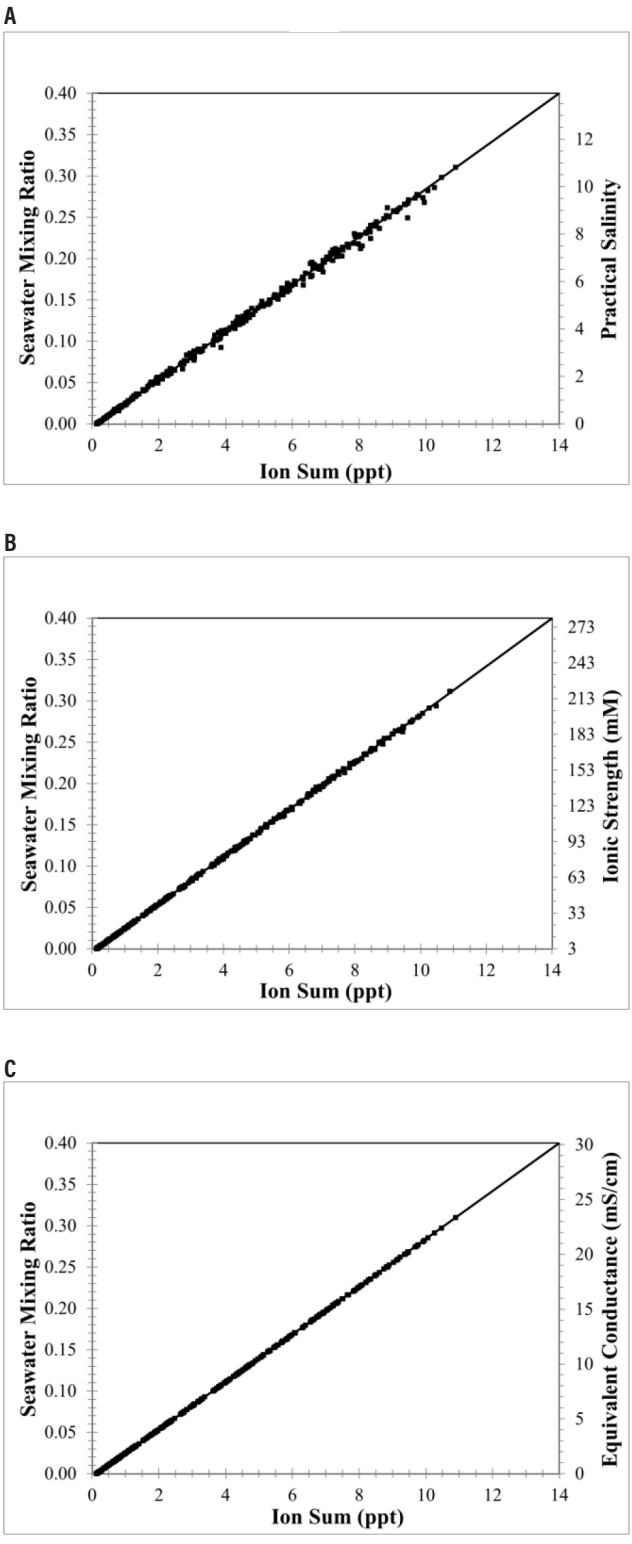

Figure 3 Seawater mixing ratio vs. ion sum. Panels (**A**), (**B**) and (**C**) overlay practical salinity, measured ionic strength and limiting equivalent conductance values, respectively. Data are shown as *points*; mixing ratios are shown as *lines*.

Source-Specific Correlations Between Bulk Salinity Measures and EC

Confirmation of EC deviation from steady-state, conservative mixing behavior motivated further work on the use of previously identified bulk salinity measures as model constituents for transport studies in the estuary. Specifically, we evaluated their respective correlations with EC among the dominant source waters in the study area. Without consistent correlations, data translations between EC and the bulk salinity measures must account for complex source-water mixing in the study area. With prior knowledge that the study area's source waters have unique anion and cation signatures, we restricted our evaluation to bulk salinity measures (i.e., we did not consider individual ions as potential model constituents).

Figure 4 plots the three bulk salinity measures as functions of EC for each of the dominant source waters in the study area. The top, middle, and bottom panels show the EC correlation with practical salinity, ionic strength, and limiting equivalent conductance, respectively. To enhance chart readability, seawater relationships are shown as predicted curves rather than as measured data; these predicted curves are based on modeled relationships between ionic concentrations and EC that were derived through an extension of the PSS-78 scale (Hutton and Roy 2023b).

Correlations Between Practical Salinity and EC

The predicted seawater relationship between PSS-78 and EC in the top panel of Figure 4 follows Equation 4. Consistent with the findings reported by Hutton and Roy (2023a, 2023b), the predicted seawater relationship overlays data for the Sacramento River—the largest riverine input to the estuary—but underestimates salinity in waters dominated by the San Joaquin River and agricultural drainage. Thus, converting between EC and practical salinity data within the context of transport model simulation, calibration, and validation must account for complex temporal and spatial variation in source-water mixing within the estuary. Hutton and Roy (2023a, 2023b) also provide inverse relationships to predict EC as a

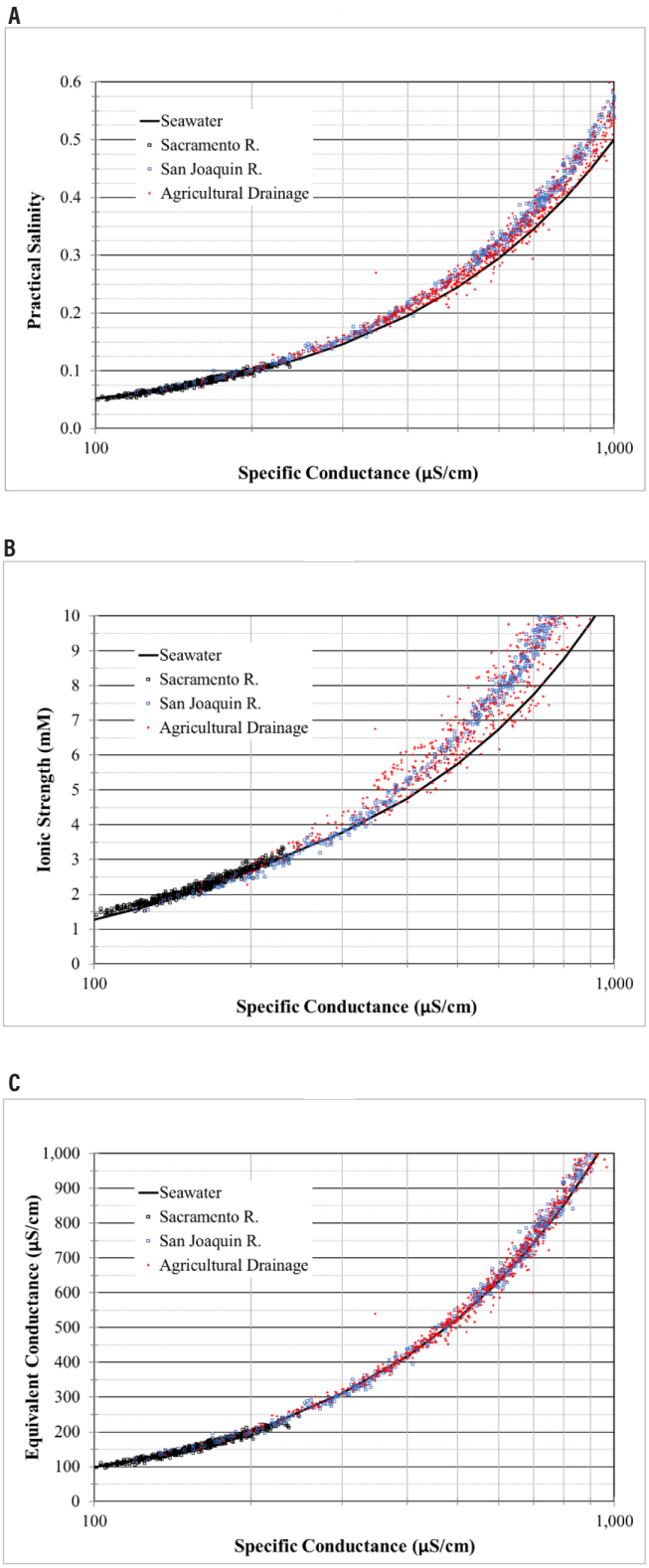

Figure 4 Relationships between specific conductance and practical salinity, ionic strength, and limiting equivalent conductance are shown for estuarine water sources in panels (**A**), (**B**), and (**C**), respectively.

function of practical salinity for the study area's source waters.

Correlations Between Ionic Strength and EC

The predicted seawater relationship between ionic strength and EC in the middle panel of Figure 4 underestimates ionic strength in all upstream source waters in the study area. Visual inspection of the panel suggests that (1) correlations between ionic strength and EC are subject to greater variance than practical salinity, and (2) deviations with the predicted seawater relationship are greater than for practical salinity. Thus, converting between EC and ionic strength data within the context of transport model simulation, calibration, and validation must account for complex temporal and spatial variation in source-water mixing within the estuary. Poorer correlation between ionic strength and EC suggests that ionic strength would be inferior to practical salinity as a transport-model constituent. Derivation of an equation that predicts ionic strength as a function of the conductivity ratio R is provided in Appendix A.

Correlations Between Limiting Equivalent Conductance and EC

The predicted seawater relationship between limiting equivalent conductance and EC in the bottom panel of Figure 4 aligns well with all dominant source waters in the study area. However, we note that visual inspection of the panel suggests some limited tendency of the predicted seawater relationship to underpredict κ at EC values greater than 800 µS cm^{-1}. Thus, it appears that converting between EC and κ data within the context of transport model simulation, calibration, and validation can ignore temporal and spatial variation in source water mixing with little error.

Predicting Limiting Equivalent Conductance from EC

A limiting equivalent conductance ratio can be computed as a function of the conductivity ratio R (and thus EC) through the following relationship:

https://doi.org/10.15447/sfews.2023v21iss2art3

$$\frac{\kappa}{\kappa_s} = L_0 + L_1 * R^{0.5} + L_2 * R + L_3 * R^{1.5} + L_4 * R^2 + L_5 * R^{2.5} \quad (7)$$

where κ is limiting equivalent conductance, κ_s is the limiting equivalent conductance of seawater (75,636 µS cm^{-1}), L_o = 0.0003, L_1 = –0.0062, L_2 = 0.7237, L_3 = 0.3935, L_4 = - 0.1851, L_5 = 0.0738, $\sum L$ = 1, and R is the conductivity ratio as previously defined. Equation 7 is derived by substituting into Equation 6 functional relationships between ion concentrations and R as presented elsewhere (Hutton and Roy 2023b); these functional relationships depend on PSS-78 constants and end-member concentrations associated with each ion. Derivation of Equation 7 is provided in Appendix B. Hutton and Roy (2023b) report adjustments to these relationships under low-salinity conditions when EC < 250 µS cm^{-1}, stating that "under such conditions, waters in the study area overwhelmingly reflect characteristics of upstream freshwater flows and do not reflect seawater mixing." As a simplifying assumption, we set κ = EC when EC < 250 µS cm^{-1}.

Conductivity-based estimates of κ from Equation 7 align very closely with mass-based estimates from Equation 6. The top panel of Figure 5, which presents a scatter plot that compares the two estimates, shows close alignment along the 1:1 line. The bottom panel of Figure 5 presents a frequency analysis of differences between conductivity-based estimates and mass-based estimates. Seventy-five percent of the conductivity-based estimates fall within ±3% of the mass-based estimate; nearly 90% of the conductivity-based estimates fall within ±5% of the mass-based estimates. Although not formally evaluated, the residuals appear to be normally distributed.

We generated model constants for an inverse formulation of Equation 7 as a function of limiting equivalent conductance ratio:

$$R = L_0' + L_1' * \left(\frac{\kappa}{\kappa_s}\right)^{0.5} + L_2' * \frac{\kappa}{\kappa_s} + L_3' * \left(\frac{\kappa}{\kappa_s}\right)^{1.5} + L_4' * \left(\frac{\kappa}{\kappa_s}\right)^{2} + L_5' * \left(\frac{\kappa}{\kappa_s}\right)^{2.5} \quad (8)$$

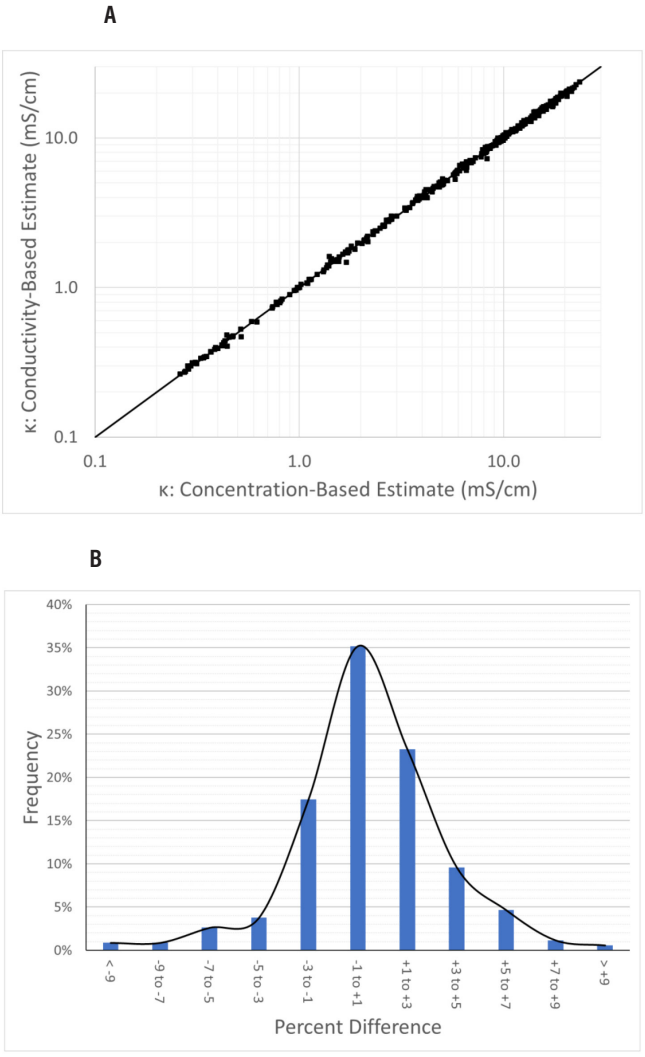

Figure 5 Comparison of conductance-based and concentration-based estimates of limiting equivalent conductance (µS cm^{-1}). Panel (**A**) compares estimates along a 1:1 line. Panel (**B**) shows the frequency of differences.

where values of L_o' = - 0.0008, L_1' = 0.0207, L_2' = 1.2812, L_3' = - 0.4780, L_4' = 0.2575, L_5' = –0.0807, and $\sum L'$ = 1.0. As a simplifying assumption, we set EC = κ when κ < 250 µS cm^{-1}.

Quantifying the Effect of EC Deviations from Conservative Mixing Behavior

Earlier, we demonstrated that, although measured EC deviates from steady-state conservative mixing behavior, κ does not. Here, we attempt to quantify how this deviation affects salinity transport modeling results when EC is used as a transport

constituent thru evaluation of (1) synthetic mixing ratio data and (2) hydrodynamic modeling results.

Evaluation of Synthetic Mixing Ratio Data

We synthetically generated two EC data sets that spanned the salinity gradient from 100% seawater (M_n = 1.0) to 100% freshwater (M_n = 0.0) assuming steady-state, two-source, conservative mixing and end- member values presented in Table 3. The first data set, denoted as "computed," was generated assuming κ end-member values that ranged from 75,636 to 259 µS cm^{-1} and then translated to EC values with Equation 8. The second data set, denoted as "measured," was generated assuming EC end-member values that ranged from 52,300 to 250 µS cm^{-1}. These synthetically generated data sets are plotted in Figure 6A with M_n on the y-axis and EC on the x-axis. Noting that the "computed" data curve always lies below the "measured" data curve, and recalling that κ follows conservative mixing assumptions, Figure 6A confirms our earlier assertion that using EC as a measure of transport in the estuary artificially amplifies the actual seawater mixing ratio—i.e., it suppresses the dilution effect associated with freshwater flows to the estuary. Figure 6B shows the same data sets as the top panel; however, the axes are interchanged and shown as log scales. The bottom panel also presents percent difference on a secondary ordinate. This panel shows that "measured" values are consistently lower than "computed" values for a given mixing ratio, and that percent differences reach a maximum of approximately 25% in the measured range of 1,300 to 1,600 µS cm^{-1}. Differences are ≥20% in the measured range of 600 to 5,400 µS cm^{-1}.

We hypothesized that Figure 6, which assumes an ocean tidal boundary, overstates the effect of EC non-conservative behavior in modeling domains that are structured with a more upstream tidal boundary. For example, the DSM2 hydrodynamic model (CDWR 2022) is structured with a tidal boundary at Martinez, which is 55 km upstream of the estuary's seawater boundary at Golden Gate (Figure 1). To test this hypothesis, we redefined M_n from a seawater mixing ratio to a "Martinez" mixing ratio by substituting the seawater end-

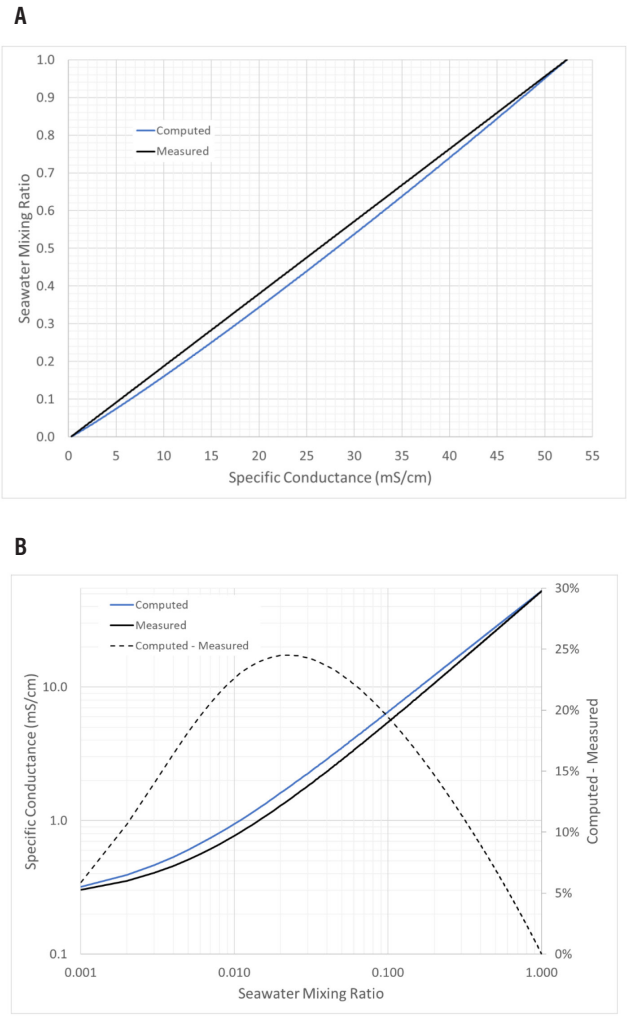

Figure 6 Panels (**A**) and (**B**) compare two synthetically generated specific-conductance data sets that span the salinity gradient from 100% seawater (Mn = 1.0) to 100% freshwater (Mn = 0.0) assuming steady-state, two-source, conservative mixing and end-member values presented in Table 3. The first data set, denoted as "computed," was generated assuming κ end-member values that ranged from 75,636 to 259 µS cm^{-1} and then translated to conductance values with Equation 8. The second data set, denoted as "measured," was generated assuming conductance end-member values that ranged from 52,300 to 250 µS cm^{-1}.

member conductivity of 52,300 µS cm^{-1} with 25,000 µS cm^{-1} in Equation 2, a conductivity that roughly corresponds with an antecedent outflow of 5,200 cfs at Martinez (Hutton et al. 2016). Following Figure 2, observed data were re-plotted in Figure 7, assuming the redefined value of M_n; this figure, in fact, shows a lesser deviation

https://doi.org/10.15447/sfews.2023v21iss2art3

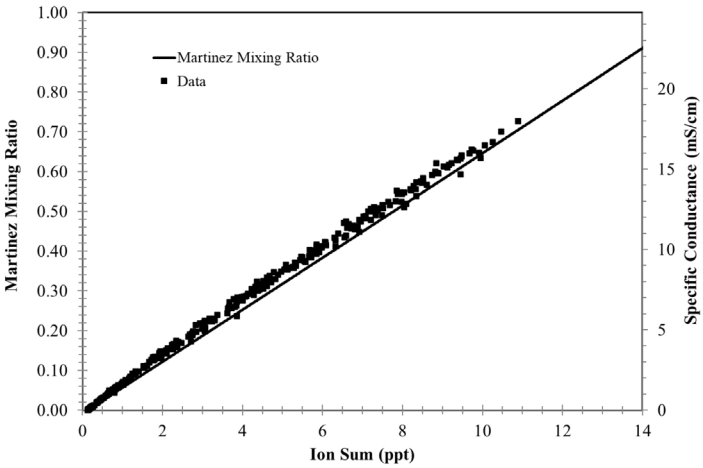

Figure 7 Martinez mixing ratio vs. ion sum. The chart overlays specific conductance data (mS/cm) measured at Martinez as a function of ion sum.

between data and the conservative mixing curve. The synthetic data analysis described above was repeated with re-defined M_n values. Similar to the previous analysis, "measured" values are consistently lower than "computed" values for a given mixing ratio. As we hypothesized, the effect of EC non-conservative behavior is lower in a modeling domain that is structured with a more upstream tidal boundary. Percent differences reach a maximum of approximately 17% in the measured range of 900 to 1,600 µS cm^{-1}, and are ≥15% in the measured range of 600 to 2,600 µS cm^{-1}.

Evaluation of Hydrodynamic Model Data

Following the methodology outlined earlier, we found that hydrodynamic model data generated by DSM2 (CDWR 2022) were biased in their ionic relationships with EC in the vicinity of the confluence of the Sacramento and San Joaquin rivers, and downstream. Specifically, when ionic constituents and TDS were directly simulated, the model consistently overestimated their concentrations relative to EC. Furthermore, we found that this model bias propagated upstream of the confluence into the San Joaquin, Old, and Middle rivers under simulated conditions of seawater intrusion. Figure 8 provides a typical comparison of average daily DSM2-simulated concentrations of TDS, Cl^- and Na^+ along the San Joaquin River at Antioch (Figure 1) with concentrations computed from average daily simulated EC values (Hutton and Roy 2023b). For simulated EC values > 1,000 µS cm^{-1}, simulated concentrations exceeded computed concentrations by 18%, 20%, and 19% on average for TDS, Cl^- and Na^+, respectively. This finding collaborates our finding from steady-state, conservative mixing analyses—i.e., using EC as a measure of transport in the estuary artificially suppresses the dilution effect associated with freshwater flows to the estuary. We hypothesize that the magnitudes of DSM2 dispersion factors, calibrated with non-conservative EC data, are too low in the vicinity of the confluence of the Sacramento and San Joaquin rivers, and downstream, to correctly simulate conservative transport.

SUMMARY AND DISCUSSION

Our findings are summarized as follows:

- Conservative behavior of three bulk measures of salinity—practical salinity, ionic strength, and limiting equivalent conductance—was demonstrated assuming two-source, steady-state mixing. Following the same approach, deviation from conservative behavior was demonstrated for specific conductance. Using EC as a measure of transport in the estuary artificially amplifies the actual seawater mixing ratio. Or, said another way, it suppresses the dilution effect associated with freshwater flows to the estuary.

- DSM2, a one-dimensional hydrodynamic model for the estuary, was shown to provide biased relationships between EC and ionic constituents. We hypothesize that this bias is a result of the model's dispersion factors being calibrated with a non-conservative constituent (i.e., EC).

- Following Hutton and Roy (2023b), this work demonstrates that the relationship between practical salinity and EC is source-specific. Thus, converting between EC and practical salinity data within the context of transport model simulation, calibration, and validation

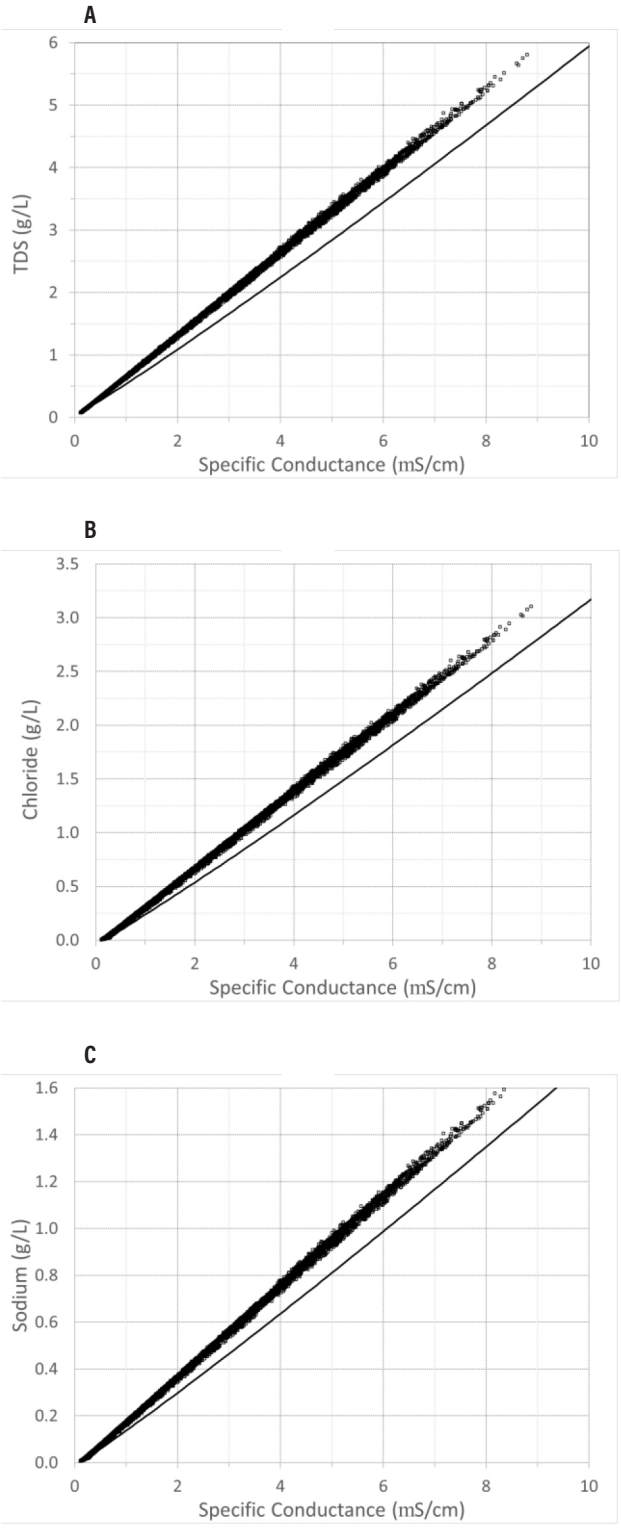

Figure 8 Comparison of DSM2-simulated and observed relationships between ionic concentrations (g L^{-1}) and specific conductance (mS cm^{-1}) at Antioch. Panels (**A**), (**B**) and (**C**) show relationships with TDS, chloride, and sodium, respectively. Simulated and observed relationships are shown as *points* and *lines*, respectively. Observed relationships based on Hutton and Roy (submitted).

must account for complex temporal and spatial variation in source-water mixing within the estuary. Similarly, the relationship between ionic strength and EC is source-specific.

- The relationship between limiting equivalent conductance and EC aligns well with all dominant source waters in the study area. Thus, converting between EC and κ data within the context of transport model simulation, calibration, and validation can ignore temporal and spatial variation in source-water mixing with little error.

Specific conductance is used as the primary salinity-transport constituent for some hydrodynamic models of the estuary (including DSM2), recognizing a practical trade-off between errors of data translation and model simulation. This approach requires no data translation, as measured EC is used directly in model calibration, validation, and scenario simulation. While such an approach potentially incorporates non-conservative behavior through manipulation of dispersion factors, the resulting calibration introduces bias in the simulation of other conservative constituents. We recommend that this trade-off in calibration using a non-conservative constituent vs. a true conservative constituent be considered more explicitly. Although the issue of non-conservative behavior is expected to be most consequential in the calibration of mechanistic water-quality models (such as DSM2) and "hybrid" mechanistic–empirical model emulators (e.g., Chen et al. 2018) built around mass balance, there may also be advantages to revisiting the calibration of purely empirical flow–salinity estuarine models (Denton 1993; Hutton et al. 2016).

A casual review of the literature reveals that practical salinity is the most utilized salinity-transport constituent in estuarine hydrodynamic models. Using practical salinity for the estuary has the advantages of providing conservative behavior and easily understandable mass balance, in addition to the advantage of aligning with standard practice. However, the use of practical salinity introduces the potential for significant

https://doi.org/10.15447/sfews.2023v21iss2art3

data translation error, particularly within the interior Delta region of the study area. Hutton and Roy (2023a, 2023b) have shown that the unique ionic make-up of waters dominated by the San Joaquin River and agricultural drainage results in varying relationships between practical salinity and EC in the study area. This behavior is compounded by the fact that source-water dominance varies spatially and temporally as a result of complex hydrodynamics within the Delta.

We believe that limiting equivalent conductance provides a credible alternative to practical salinity as a salinity-transport constituent in estuarine hydrodynamic modeling. κ provides conservative behavior and, at least for the estuary, has a source-independent relationship with EC, and thus minimizes issues related to data-translation error. Simulation results could easily be translated from κ, a theoretical quantity, to a more standard output such as EC or practical salinity for scenario analysis. We recommend that adoption of this approach be evaluated in further detail in the San Francisco Estuary as well as for other estuaries that are influenced by multiple source waters of varying ionic makeup.

ACKNOWLEDGEMENTS

This work was made possible through funding from the State Water Contractors. The authors acknowledge Arushi Sinha's contribution to this work through data assembly and screening. We thank John Rath for performing the DSM2 runs in support of this analysis.

REFERENCES

[CDWR] California Department of Water Resources. 2022. DSM2: Delta Simulation Model II. [accessed 2023 Apr 5]. Available from: *https://water.ca.gov/Library/Modeling-and-Analysis/Bay-Delta-Region-models-and-tools/Delta-Simulation-Model-II*

Chen L, Roy SB, Hutton PH. 2018. Emulation of a process-based estuarine hydrodynamic model. Hydrol Sci J. 63(5):783–802. *https://doi.org/10.1080/02626667.2018.1447112.*

[DSC] Delta Stewardship Council. 2021. The Delta plan. [accessed 2023 Apr 5]. Available from: *https://deltacouncil.ca.gov/delta-plan/*

Denton RA. 1993. Accounting for antecedent conditions in seawater intrusion modeling—applications for the San Francisco Bay–Delta. In: Hydraulic engineering. ASCE. p. 448–453. [accessed 2023 Apr 5]; *https://cedb.asce.org/CEDBsearch/record.jsp?dockey=0083891*

Denton RA. 2015. Delta Salinity Constituent Analysis. [accessed 2023 Apr 5]; *https://www.baydeltalive.com/assets/588ee18bdb51ef1619ac6fd28b97f694/application/pdf/Denton_2015_Delta_Salinity_Constituents_Report.pdf*

Fox JP, Mongan TR, Miller WJ. 1990. Trends In Freshwater Inflow to San Francisco Bay from Tue [sic] Sacramento–San Joaquin Delta. JAWRA J Am Water Resour Assoc. [accessed 2023 Apr 5];26(1):101–116. *https://doi.org/10.1111/j.1752-1688.1990.tb01355.x*

Fujii R, Ranalli AJ, Aiken GR, Bergamaschi BA. 1998. Dissolved organic carbon concentrations and compositions, and trihalomethane formation potentials in waters from agricultural peat soils, Sacramento–San Joaquin Delta, California: Implications for drinking-water quality. [Sacramento (CA)]: US Department of the Interior, US Geological Survey. [accessed 2023 Apr 5]. Available from: *https://pubs.usgs.gov/wri/wri984147/*

Hem JD. 1985. Study and interpretation of the chemical characteristics of natural water. [accessed 2023 Apr 5]. [Alexandria (VA)]: Department of the Interior, US Geological Survey. *https://doi.org/10.3133/wsp2254*

Hill K, Dauphinee T, Woods D. 1986. The extension of the Practical Salinity Scale 1978 to low salinities. IEEE J Oceanic Eng. [accessed 2023 Apr 5]; 11(1):109–112. *https://doi.org/10.1109/JOE.1986.1145154*

Hutton PH, Rath JS, Chen L, Ungs MJ, Roy SB. 2016. Nine decades of salinity observations in the San Francisco Bay and Delta: modeling and trend evaluations. J Water Resour Plan Manag. [accessed 2023 Apr 5]; 142(3). *https://doi.org/10.1061/(asce)wr.1943-5452.0000617*

Hutton PH, Roy SB. 2023a. Application of the practical salinity scale to the waters of San Francisco Estuary. Est Coast Shelf Sci. 290(5 Sep 2023):108380. *https://doi.org/10.1016/j.ecss.2023.108380*

Hutton PH, Roy SB. 2023b. Extension of the practical salinity scale to estimate major ion concentrations: application to the San Francisco Estuary. Estuaries Coasts. *https://doi.org/10.1007/s12237-023-01211-z*

Hutton PH, Roy SB, Krasner SW, Palencia L. 2022. The Municipal Water Quality Investigations Program: a retrospective overview of the program's first three decades. Water. [accessed 2023 Apr 5];14(21):3426. *https://doi.org/10.3390/w14213426*

Hutton PH, Sinha A, Roy SB. 2022. Simplified approach for estimating salinity constituent concentrations in the San Francisco Estuary and Sacramento–San Joaquin River Delta: a user guide. [accessed 2023 Apr 5]. Available from: *https://rtdf.info/public_docs/Miscellaneous%20RTDF%20Web%20Page%20Information/Other%20MWQP%20and%20DWR%20Publications/2022-07-21%20MWQI%20Conservative%20Constituents%20User%20Guide_formatted.pdf*

Lewis E. 1980. The Practical Salinity Scale 1978 and its antecedents. IEEE J Oceanic Eng. [accessed 2023 Apr 5];5:3–8. *https://doi.org/10.1109/JOE.1980.1145448*

Lewis GN, Randall M. 1921. The activity coefficient of strong electrolytes. J Am Chem Soc. [accessed 2023 Apr 5];43(5):1112–1154. *https://doi.org/10.1021/ja01438a014*

Lind CJ. 1970. Specific conductance as a means of estimating ionic strength. [Washington, D.C.]: US Geological Survey Professional Paper 700-D. p. 272–280.

Loder TC, Reichard RP. 1981. The dynamics of conservative mixing in estuaries. Estuaries. [accessed 2023 Apr 5];4(1):64–69. *https://doi.org/10.2307/1351543*

Lund JR. 2016. California's agricultural and urban water supply reliability and the Sacramento–San Joaquin Delta. San Franc Estuary Watershed Sci. [accessed 2023 Apr 5];14(3). *https://doi.org/10.15447/sfews.2016v14iss3art6*

MacWilliams ML, Ateljevich ES, Monismith SG, Enright C. 2016. An overview of multi-dimensional models of the Sacramento–San Joaquin Delta. San Franc Estuary Watershed Sci. [accessed 2023 Apr 5];14(4). *https://doi.org/10.15447/sfews.2016v14iss4art2*

McCleskey BB, Nordstrom KK, Ryan JN. 2012. Comparison of electrical conductivity calculation methods for natural waters. Limnol Oceanogr Methods. [accessed 2023 Apr 5];10:952–967. *https://doi.org/10.4319/lom.2012.10.952*

Miller RL, Bradford WL, Peters NE. 1988. Specific conductance: theoretical considerations and application to analytical quality control. [accessed 2023 Apr 5]. US General Publications Office. US Geological Survey Report. Water Supply Paper 2311. *https://doi.org/10.3133/wsp2311*

Millero FJ, Feistel R, Wright DG, McDougall TJ. 2008. The composition of standard seawater and the definition of the reference-composition salinity scale. Deep Sea Res 1 Oceanogr Res Pap. [accessed 2023 Apr 5];55(1):50–72. *https://doi.org/10.1016/j.dsr.2007.10.001*

Patra S, Liu CQ, Wang FS, Li SL, Wang BL. 2012. Behavior of major and minor elements in a temperate river estuary to the coastal sea. Intl J Environ Sci Technol. [accessed 2023 Apr 5];9(4):647–654. *https://doi.org/10.1007/s13762-012-0097-8*

Pawlowicz R. 2008. Calculating the conductivity of natural waters. Limnol Oceanogr Methods. [accessed 2023 Apr 5];6(9):489–501. *https://doi.org/10.4319/lom.2008.6.489*

Riley JP, Skirrow G, 1965. Chemical oceanography. Volume 1. London and New York: Academic Press.

Schemel LE. 2001. Simplified conversions between specific conductance and salinity units for use with data from monitoring stations. Interagency Ecological Program Newsletter. 14:17–18. [accessed 2023 Apr 5]. Available from: *https://pubs.er.usgs.gov/publication/70174311*

Warner TB. 1972. Mixing model prediction of fluoride distribution in Chesapeake Bay. J Geophys Res. [accessed 2023 Apr 5];77(15):2728–2732. *https://doi.org/10.1029/jc077i015p02728*